Available online at www.sciencedirect.com
SCIENCE DIRECT®
Journal of Magnetic Resonance 173 (2005) 23–28
JMR Journal of Magnetic Resonance
www.elsevier.com/locate/jmr

NMR detection and one-dimensional imaging using the inhomogeneous magnetic field of a portable single-sided magnet

S. Rahmatallah[a,1], Y. Li[a,b,1], H.C. Seton[c,*], I.S. Mackenzie[d], J.S. Gregory[a], R.M. Aspden[a]

[a] Department of Orthopaedics, IMS Building, Medical School, University of Aberdeen, Foresterhill, Aberdeen AB25 2ZD, UK
[b] Radiological Sciences Unit, 2nd Floor, Neptune Building, Imaging Sciences Department, Hammersmith Hospital, Du Cane Road, London W12 0HS, UK
[c] Department of Bio-Medical Physics and Bio-Engineering, University of Aberdeen, Foresterhill, Aberdeen AB25 2ZD, UK
[d] Department of Physics, Fraser Noble Building, University of Aberdeen, Aberdeen AB24 3UE, UK

Received 20 July 2004; revised 10 November 2004
Available online 8 December 2004

Abstract

A portable, nuclear magnetic resonance (NMR) probe is described which utilises the intrinsic inhomogeneity of the field produced by a single-sided magnet to provide spatial encoding of the NMR signal. The probe uses a longitudinally magnetised hollow cylinder, and a figure-8 radiofrequency (RF) surface coil. The system has been used to measure NMR relaxation times and one-dimensional NMR profiles of rubber phantoms.

Keywords: Inhomogeneous; Profile; Relaxation; Portable

1. Introduction

In a conventional nuclear magnetic resonance (NMR) experiment efforts are made to achieve homogeneity of the static magnetic field, B_0, and the radiofrequency (RF) field, B_1, over the sample volume. This normally requires that the sample is positioned inside the NMR apparatus. In recent years, however, a significant body of work has been published on the development of low cost NMR systems for specialised applications. Some of these use relatively inhomogeneous fields produced by single-sided magnets, which remove many of the restrictions on, for example, sample size, imposed by the geometry of standard NMR instruments.

STRAFI is a one-dimensional (1-D) NMR imaging technique that employs the strong axial gradient in the stray field at the ends of a standard high field superconducting magnet [1]. A thin slice of the sample, perpendicular to the gradient direction, is selectively excited with a suitably shaped RF pulse. A 1-D profile is obtained by mechanically stepping the sample through the selectively excited region. In another variation, Blümich et al. [2] have developed the NMR mobile universal surface explorer (MOUSE) as a portable NMR tool for non-invasive measurements of material properties. In its original form the NMR MOUSE was based around two anti-parallel permanent magnets, positioned on an iron yoke, to form a horseshoe geometry [3–6]. An RF coil was positioned in the air gap between the permanent magnets to excite and detect the NMR signal. More recently, this group has used an alternative magnet geometry in which the B_0 field is generated near one pole face of a single, magnetised rectangular or cylindrical block, which also carries an RF surface coil [7–10]. This system has been used, together with a pulsed gradient system, to generate 2-D cross-sectional images [9]. Other single-sided NMR devices include one with

* Corresponding author.
E-mail address: h.seton@biomed.abdn.ac.uk (H.C. Seton).
[1] These authors contributed equally.

1090-7807/$ - see front matter © 2004 Elsevier Inc. All rights reserved.
doi:10.1016/j.jmr.2004.11.014

the main field generated by an array of magnetised blocks, which has been used to monitor the moisture content of concrete, porous rocks, and wood [11,12].

This paper presents a new portable NMR probe, which combines some aspects of these existing techniques, but which can also be used to obtain 1-D profiles without the need to move the sample or re-tune the RF coil. The magnet is similar to that described by Fukushima [13], except that instead of being homogeneous, the field it produces has a controlled inhomogeneity that enables some spatial localisation without the use of gradient coils, retuning the RF coils or moving the sample. The new device has potential applications in many areas including dermatology and the food industry.

2. The probe system

2.1. Permanent magnet design, construction, and simulation

"Single-sided" NMR inevitably suffers from inhomogeneous B_0 and B_1 fields. The challenge is to extract useful information from the NMR measurement despite the complex interplay of these fields which leads to variable excitation efficiency and sensitivity across the sample volume. Generally, the signal-to-noise ratio increases with the magnitude of B_0 so there is a premium on achieving a high value, although this presents a potential hazard in portable systems that may be moved close to other magnetic materials.

Potential magnet geometries were modelled and evaluated using commercial finite element (FE) software (ANSYS, Canonsburg, PA, USA). In this paper, we present the results for an axially magnetised, hollow cylinder. This geometry produces a saddle point in the magnetic field beyond the face of the cylinder, which can be used to define a region of interest for measurements within an extended sample, and also a point of inflexion in the axial field beyond the maximum (see Fig. 1), which is advantageous for 1-D profiling. The parameters of the magnet are: inner and outer radii 7.5 and 50 mm, length 90 mm, and mass 5.18 kg. The magnet was constructed commercially (Sura Magnets, Sweden) from two 45 mm-long magnetised cylinders, held together by mutual attraction. The magnets are made from neodymium iron boron (NdFeB), chosen for its high energy product and relative ease of manufacture into a variety of shapes.

Magnetic field components were measured using a Hall probe (type GM04, Hirst Magnetic Instruments, UK). Fig. 1 shows the experimental and FE-modelled variation of the axial (z)-component of the B_0 field along the magnet's axis, together with the axial derivative of the simulated variation. The field reaches a maximum

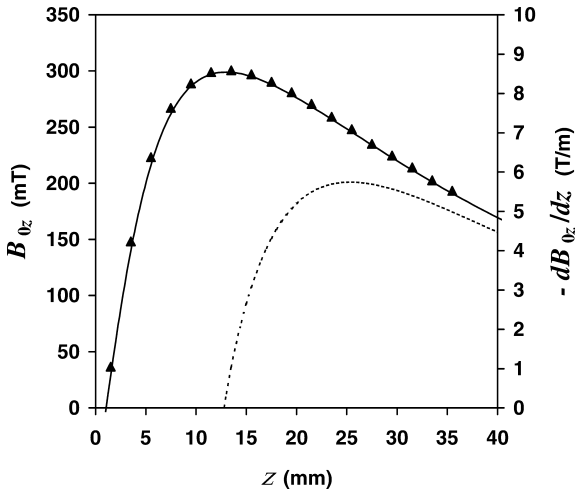

Fig. 1. Measured (points) and modelled (solid curve) variation of the axial magnetic flux density, B_{0z}, along the z-axis of the axially magnetised hollow cylinder and the derivative, $-\mathrm{d}B_{0z}/\mathrm{d}z$, of the simulated curve (dashed curve). The origin is at the magnet face, and the centre of the magnet is located at $z = -45$ mm.

of approximately 0.30 T at 13.5 mm from the magnet face, and then falls off with increasing distance. However, we are primarily interested in the region beyond the peak where the gradient in B_{0z} may be used as the basis for obtaining a 1-D profile of the sample in the z-direction.

One-dimensional imaging in a static field ideally requires a region of uniform magnetic field gradient in the direction of the desired profile. In the case of axial symmetry the best approximation to this is at the point of inflexion of the B_{0z} field which, in the present case, occurs at about 24 mm from the magnet face. Outside the magnet, in regions containing no magnetic materials, $\nabla \cdot \boldsymbol{B} = 0$ and $\nabla \times \boldsymbol{B} = 0$, so that on the cylindrical axis it follows that

$$\frac{\partial B_{0z}}{\partial r} = 0 \tag{1}$$

and

$$\frac{\partial^2 B_{0z}}{\partial z^2} = -2\frac{\partial^2 B_{0z}}{\partial r^2}. \tag{2}$$

Eqs. (1) and (2) indicate that the point of inflexion of the axial field variation (Fig. 1) is a favourable location for 1-D imaging, since regions where the axial curvature in B_{0z} is zero also have no radial curvature, with the result that B_{0z} is constant to second order in the radial direction. The best position for 1-D profiling depends on the lateral extent of the desired sensitive region and may differ slightly from the point of inflexion. In the present case, the field at the point of inflexion is 255 mT and the gradient is 5.7 T/m. The importance of the gradient in relation to the attainable field of view will be discussed below.

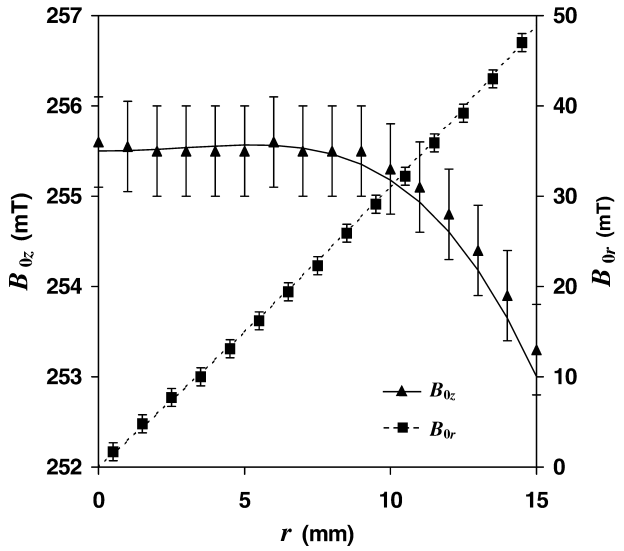

Fig. 2. Measured (points) and modelled (curves) radial variation of the axial, B_{0z}, and radial, B_{0r}, magnetic flux density components at 24 mm from the magnet face.

Fig. 2 plots the radial dependence of the axial, B_{0z}, and radial, B_{0r}, field components (again showing both measured and FE-modelled data) at an axial displacement of 24 mm. The B_{0z} component is seen to be constant to within ±0.2 mT of 255.5 mT out to a radius of 7.5 mm, while the B_{0r} component varies from zero on-axis to 23 mT at 7.5 mm radius. The test measurements reported in this paper were conducted on samples located approximately 24 mm from the magnet face, where the field has a strong axial gradient but only a small radial dependence.

2.2. RF system

To achieve a B_1 field normal to B_0 the system employs a 27 mm diameter figure-8 transmit–receive surface coil, shown in Fig. 3, with its plane parallel with the magnet face, similar to that described previously [8]. This is formed from two 10-turn, D-shaped loops of plastic-insulated copper wire, with a conductor diameter of 0.25 mm. The loops are counter-wound as this gives a measure of protection against interference fields. This is an important consideration in applications where additional RF shielding is impractical [14]. The relatively poor depth performance of this configuration was not a problem in this instance as the field gradient and frequency bandwidth restrict the depth of the sensitive volume.

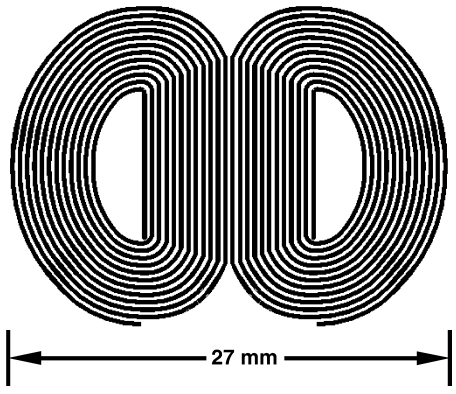

Fig. 3. The figure-8 surface coil.

The plane of the RF coil is parallel to the magnet face with its upper surface 23.5 mm above the magnet. It is separated from the sample by a 0.5 mm glass slide. In this region the proton resonance frequency is approximately 10.9 MHz. The coil inductance, of 0.55 μH, was tuned to this frequency and matched to a 50 Ω coaxial cable with low loss capacitors. The matched Q-factor was measured to be 40, and the field per unit current, B_1/I, produced at the centre of the sample region was found to be about 0.7 mT/A.

A commercial console was used to generate NMR pulse sequences and acquire data (SMIS/MRRS, Guildford, Surrey, UK). Rectangular RF pulses, of 1–5 μs duration, were delivered to the coil, via a passive transmit-receive switch, from a 250 W RF amplifier (Type BT00250-CLB, Tomco Electronics Pty, Norwood, Australia).

3. Methods and results

In this section are reported some simple experiments that were used for evaluation of the probe. In NMR measurements on extended samples the strength of the signal may be of interest in itself, e.g. in monitoring the time evolution of water content. However, given the versatility of the NMR method, it is likely that measurements of dynamic aspects of the signal will play a significant role in applications. To that end we have monitored the response from an extended sample to conventional pulse sequences for T_1 and T_2 measurement.

It has to be acknowledged that the response to conventional sequences, which depend on the local tipping angle achieved and the effectiveness of a refocusing 180° pulse, will be corrupted to some extent by the imperfect relationship between B_1 and B_0 in the inhomogeneous fields [15]. The extent of these effects is being investigated by computer simulation.

3.1. Relaxation rate measurements

Samples were prepared from two types of rubber. Disks approximately 1 mm thick and 6 mm diameter were cut from the white and blue ends of a pencil eraser. The NMR relaxation times of these samples were estimated using Hahn spin echo pulse sequence. The 90 and 180° RF pulse widths were fixed at 2.5 and 5 μs,

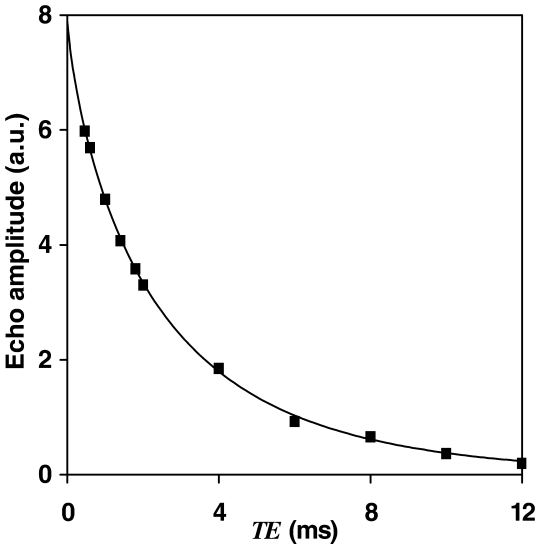

Fig. 4. Spin echo amplitude (in arbitrary units) as a function of TE for the white rubber sample, recorded with the single sided probe at 10.9 MHz and 23 °C. TR was fixed at 150 ms.

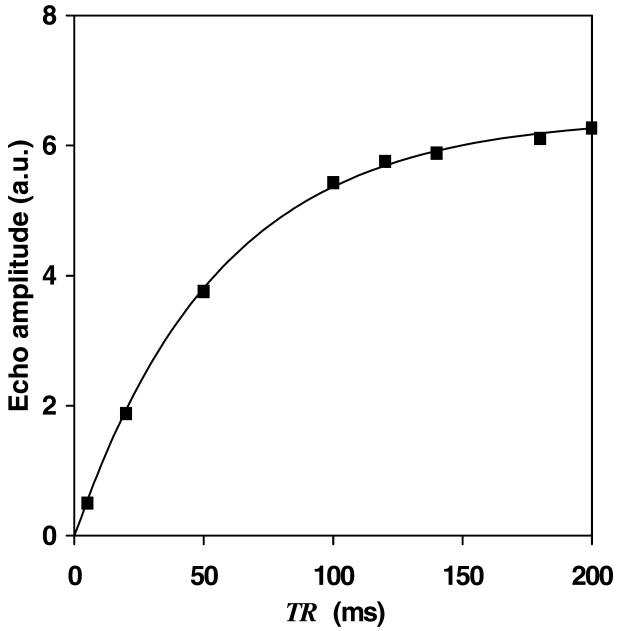

Fig. 5. Spin echo amplitude (in arbitrary units) as a function of TR for the white rubber sample, recorded with the single sided probe at 10.9 MHz and 23 °C. TE was fixed at 0.46 ms.

respectively, and the pulse amplitude was varied to maximise the echo amplitude.

To estimate T_2, the sequence repetition time, TR, was fixed at 150 ms and echo amplitudes were recorded as a function of echo time, TE. The data for the white rubber sample are shown in Fig. 4. Each point was accumulated from 1000 averages, with an acquisition time of about $2\frac{1}{2}$ min. When the data are fitted to a stretched exponential function [16] of the form $S = S_0 \exp(-(1/b)(\mathrm{TE}/T_2)^b)$, this yields a T_2 value of approximately 3.3 ms, with a b value of 0.79.

T_1 was estimated by recording echo amplitudes as TR was varied, with TE fixed at 0.46 ms, and then fitting a saturation recovery curve of the form $S = S_0(1 - \exp(-\mathrm{TR}/T_1))$ to the data. Fig. 5 shows the results, from which the white sample's T_1 was estimated to be about 57 ms. T_1 and T_2 were estimated in the same way for the blue sample to be 29 and 3.3 ms.

It needs to be noted that the use of inhomogeneous B_0 and B_1 fields complicates the experiment, so further work will be required to quantify how the relaxation times estimated by the above methods relate to the true values which would be found in uniform static and RF fields [15,17].

3.2. One-dimensional profiles

The gradient in the field, B_{0z}, near to the axial inflexion point was used to provide spatial resolution of the NMR signals. Two test objects, each with overall thickness less than 1.4 mm, were made to demonstrate the 1-D profiling capability.

The axial B_0 variation over the phantom thickness corresponds to a frequency range of about 350 kHz, so the RF excitation bandwidth, determined by RF pulse length and the RF coil's signal response, should be compatible with this range. The profiling experiments we report here utilised maximum pulse durations of 2.2 μs, corresponding to an excitation bandwidth of about 450 kHz. The coil's intrinsic Q-factor of 40 would have limited the effective bandwidth to approximately 270 kHz, so 0.5 Ω was added in series with the windings to reduce the Q-factor to approximately 20. Although this reduced the sensitivity to NMR signals, the profiling capability was improved because the full excitation bandwidth could be used.

The first phantom comprised three thin disks of the rubber materials described earlier. The disks were, as before, 6 mm diameter; one white rubber disk of thickness 0.25 mm was sandwiched between two blue disks of thickness 0.26 and 0.34 mm, with 0.27 mm glass slides used as separators.

Spin echo signals were accumulated from the phantoms over 10,000 averages, with TE fixed at 0.2 ms. TR was set first to 150 ms and then 30 ms, giving acquisition times of 25 and 5 min, to produce profiles with different T_1 weightings. Fig. 6 shows the frequency spectra of the accumulated signals for both values of TR. These spectra correspond to 1-D projections of the distribution of ^{1}H in the sample, in a direction perpendicular to the magnet face. Three peaks corresponding to the rubber disks are clearly resolved in each trace, with the left-hand peak emanating from the disk nearest the magnet and RF coil.

The particular surface coil geometry employed here is unfavourable for SNR, compared, for example, to a solenoid, but it has the important advantage of allowing

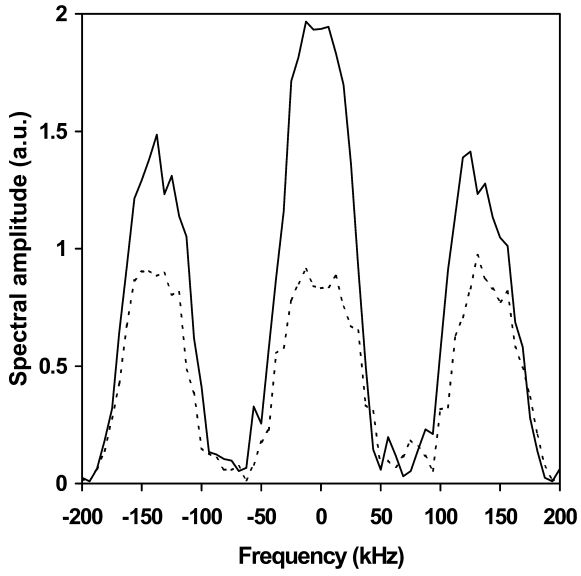

Fig. 6. NMR profiles (in arbitrary units) from a test object comprising white and blue rubber samples, recorded with the single sided probe at 10.9 MHz and 23 °C. TE was fixed at 0.2 ms for both profiles; the TR values are 150 ms (solid line) and 30 ms (dashed line).

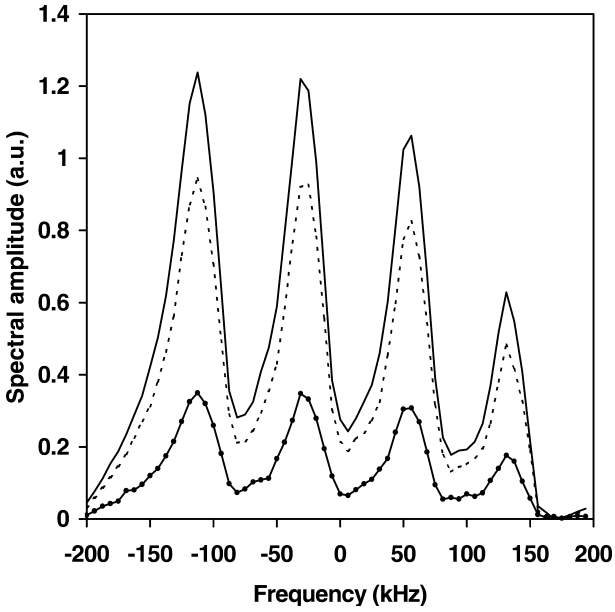

Fig. 7. NMR profiles (in arbitrary units) from a test object comprising four thin rubber sheets, recorded with the single sided probe at 10.9 MHz and 23 °C. TE was fixed at 0.2 ms; the TR values are 150 ms (solid line), 30 ms (dashed line), and 10 ms (line with points).

single-sided access for measurements on extended objects. To confirm that the sensitivity was as expected, the SNR of the profile recorded for TR = 30 ms, shown in Fig. 6, was estimated from the raw data (i.e., before Fourier transform) by comparing the spin echo amplitude with the RMS noise level, and found to be about 50. This is compatible with the value calculated by using the reciprocity principle [18] with the RF coil parameters given in Section 2.2.

There is evidence from the relative linewidths of the expected reduction in sensitivity towards the extremes of the spectrum. As has been noted, this has its roots in the complex interplay of the inhomogeneous B_0 and B_1 fields and is a crucial issue in static field 1-D profiling experiments. However the slice widths and separations confirm the preliminary Hall probe measurement of the field gradient of 5.7 T/m.

The T_1 and T_2 values reported in Section 3.1 suggest that the profile acquired with TR = 150 ms should display mainly proton density information, with very little T_1 weighting. The profile acquired with TR = 30 ms shows a reduction in the signals due to partial saturation effects. The reductions are in accordance with the measured T_1 values, the white and blue samples being reduced to 44 and 57% of their previous values. This simple experiment demonstrates the system's potential for measuring relaxation properties of materials as a function of depth.

The spatial resolution in the profile is determined by the resolution inherent in the data acquisition protocol (in this case 64 samples at 400 kHz) compounded by the radial variation in the total field, B_0, within the slice. In the frequency domain these contributions to the line broadening amount to about 6 and 8 kHz, respectively, and limit the spatial resolution to about 60 μm in the axial profiling direction. However, this phantom is wholly within the sensitive volume of the apparatus and so does not adequately test the depth resolution for an extended sample.

The second phantom is a four-layer sandwich of identical thin rubber sheets, each $25 \times 35 \times 0.13$ mm, sandwiched between 0.2 mm thick glass slides. The experimental protocol is the same as the previous one except that, because this material has a shorter T_1, an additional spectrum was obtained with TR = 10 ms. The data are shown in Fig. 7. The T_1 relaxation time deduced from the TR dependence of the spectrum is approximately 22 ms. This figure is consistent for all four layers.

This sample extends well beyond the sensitive region and demonstrates the spatial resolution attainable from extended samples. In this case, the intrinsic frequency resolution and the radial variation of B_0 contribute 6 and 20 kHz to the line broadening, the total amounting to a spatial resolution of about 110 μm, as is evidenced in Fig. 7. The higher spatial resolution for the first phantom could be achieved for an extended sample at the expense of reducing the sensitive volume by suitable tailoring of the RF field.

4. Conclusions

The potential of a new portable probe for single-sided NMR has been investigated. The longitudinally magne-

tised, cylindrical permanent magnet generates a field with an intrinsic gradient perpendicular to its end face. This has been combined with a figure-8 surface coil, which generates an RF magnetic field mainly perpendicular to the static field, to produce a single-sided NMR probe.

The probe has been used to measure relaxation rates and 1-D NMR profiles of rubber phantoms. One-dimensional profiling is achieved using the favourable region of the field gradient in the vicinity of its inflexion point and using broad-band RF excitation. The particular configuration discussed is one of a number under review and achieves a 1-D resolution of 110 μm for extended samples. This contrasts with methods reported by others which either require that the sample is moved through the field gradient [1], or that the RF excitation frequency is varied [7].

Acknowledgments

We are grateful to Scottish Enterprise for funding the project with a Proof of Concept award. We also thank the staff of the Mechanical Workshop, Department of Bio-Medical Physics and Bio-Engineering for their technical support.

References

[1] P.J. McDonald, Stray field magnetic resonance imaging, Prog. Nucl. Magn. Reson. Spectrosc. 30 (1997) 69–99.
[2] B. Blümich, P. Blümler, G. Eidmann, A. Guthausen, R. Haken, U. Schmitz, K. Saito, G. Zimmer, The NMR-MOUSE: construction, excitation, and applications, Magn. Reson. Imag. 16 (1998) 479–484.
[3] S. Anferova, V. Anferov, M. Adams, P. Blümler, N. Routley, K. Hailu, K. Kupferschläger, M.J.D. Mallett, G. Schroeder, S. Sharma, B. Blümich, Construction of a NMR-MOUSE with short dead time, Concept. Magn. Reson. (Magn. Reson. Eng.) 15 (1) (2002) 15–25.
[4] P.J. Prado, B. Blümich, Apparatus for and method of single-sided magnetic resonance imaging with palm-size probe, US patent US6, 489, 767, (2002).
[5] P.J. Prado, B. Blümich, U. Schmitz, One-dimensional imaging with a palm-size probe, J. Magn. Reson. 144 (2000) 200–206.
[6] G. Eidmann, R. Savelsberg, P. Blümler, B. Blümich, The NMR MOUSE, a mobile universal surface explorer, J. Magn. Reson. A 122 (1996) 104–109.
[7] B. Blümich, V. Anferov, S. Anferova, M. Klein, R. Fechete, M. Adams, F. Casanova, Simple NMR-MOUSE with a bar magnet, Concept. Magn. Reson. (Magn. Reson. Eng.) 15 (2002) 255–261.
[8] B. Blümich, V. Anferov, S. Anferova, M. Klein, R. Fechete, An NMR-MOUSE for analysis of thin objects, Macromolecular Mater. Eng. 288 (2003) 312–317.
[9] F. Casanova, B. Blümich, Two-dimensional imaging with a single-sided NMR probe, J. Magn. Reson. 163 (2003) 38–45.
[10] M. Klein, R. Fechete, D.E. Demco, B. Blümich, Self-diffusion measurements by a constant-relaxation method in strongly inhomogeneous magnetic fields, J. Magn. Reson. 164 (2003) 310–320.
[11] P.J. Prado, Single sided imaging sensor, Magn. Reson. Imag. 21 (2003) 397–400.
[12] P.J. Prado, NMR hand-held moisture sensor, Magn. Reson. Imag. 19 (2001) 505–508.
[13] E. Fukushima, J.A. Jackson, Unilateral magnet having a remote uniform field region, US patent US6,489,872.
[14] B.H. Suits, A.N. Garroway, J.B. Miller, Noise-immune coil for unshielded magnetic resonance measurements, J. Magn. Reson. 131 (1998) 154–158.
[15] M.D. Hürlimann, D.D. Griffin, Spin dynamics of Carr–Purcell–Meiboom–Gill-like sequences in grossly inhomogeneous B0 and B1 fields and application to NMR well logging, J. Magn. Reson. 143 (2000) 120–135.
[16] L. Zanzotto, J. Stastna, Dynamic master curves from the stretched exponential relaxation modulus, J. Polymer Sci. Part B: Polymer Phys. 35 (1998) 1225–1232.
[17] F. Balibanu, K. Hailu, R. Eymael, D.E. Demco, B. Blumich, Nuclear magnetic resonance in inhomogeneous magnetic fields, J. Magn. Reson. 145 (2000) 246–258.
[18] D.J. Hoult, R.E. Richards, The signal to noise ratio of the nuclear magnetic resonance experiment, J. Magn. Reson. 24 (1976) 71–85.